Molecular Neurobiology (2019) 56:5041–5050
https://doi.org/10.1007/s12035-018-1429-6

Amyloid β_{1-42}-Induced Rapid Zn^{2+} Influx into Dentate Granule Cells Attenuates Maintained LTP Followed by Retrograde Amnesia

Haruna Tamano[1] · Hiroki Suzuki[1] · Taku Murakami[1] · Hiroaki Fujii[1] · Paul A. Adlard[2] · Ashley I. Bush[2] · Atsushi Takeda[1]

Received: 27 August 2018 / Accepted: 13 November 2018 / Published online: 20 November 2018

Abstract

On the basis of the evidence that amyloid β_{1-42} ($A\beta_{1-42}$)-induced Zn^{2+} influx affects memory acquisition via attenuated long-term potentiation (LTP) induction, here we tested whether $A\beta_{1-42}$-induced Zn^{2+} influx affects maintained LTP in freely moving rats, resulting in retrograde amnesia. Both maintained LTP and space memory were impaired by local injection of 250 μM $ZnCl_2$ (2 μl) into the dentate gyrus, while maintained LTP was impaired by injection of either $A\beta_{1-40}$ or $A\beta_{1-42}$ (25 μM, 2 μl) into the dentate gyrus. $A\beta_{1-40}$-induced impairment of maintained LTP was rescued by co-injection of CaEDTA, an extracellular Zn^{2+} chelator, but not by co-injection of ZnAF-2DA, an intracellular Zn^{2+} chelator, suggesting that maintained LTP is impaired by $A\beta_{1-40}$ via a mechanism that may involve extracellular Zn^{2+}. In contrast, $A\beta_{1-42}$-induced impairments of maintained LTP and space memory were rescued by co-injection of either CaEDTA or ZnAF-2DA. Intracellular Zn^{2+} in dentate granule cells was rapidly increased by $A\beta_{1-42}$ injection into the dentate gyrus, but not by $A\beta_{1-40}$ injection. The block of $A\beta_{1-42}$-induced increase in intracellular Zn^{2+} by pretreatment with dexamethasone, a metallothionein inducer also rescued $A\beta_{1-42}$-induced impairment of maintained LTP. The present study indicates that $A\beta_{1-42}$-induced Zn^{2+} influx into dentate granule cells, which more readily occurs than free Zn^{2+}-induced Zn^{2+} influx, attenuates maintained LTP followed by retrograde amnesia. It is likely that controlling $A\beta_{1-42}$-induced intracellular Zn^{2+} dysregulation is a strategy for defending AD pathogenesis.

Keywords Amyloid β · Zn^{2+} · Dentate granule cell · Retrograde amnesia · Alzheimer's disease

Introduction

Cognitive activity is linked to strengthening and weakening synaptic connections between neurons that are synaptic plasticity, i.e., long-term potentiation (LTP) and long-term depression (LTD). Changes in both presynaptic and postsynaptic strength have been implicated in the mechanisms of synaptic plasticity as a cellular mechanism of memory, which have been widely studied in glutamatergic synapses in the hippocampus [1, 2]. In *N*-methyl-D-aspartate (NMDA)-receptor-mediated plasticity, Ca^{2+} influx into postsynaptic neurons through NMDA receptors plays a crucial role [3] and excess NMDA receptor activation by extracellular glutamate accumulation, i.e., glutamate excitotoxicity [4, 5], is a final common pathway for neuronal death [6, 7].

Extracellular Zn^{2+} permeates NMDA receptors and voltage-dependent Ca^{2+} channels, while extracellular Zn^{2+} preferentially passes through Ca^{2+}- and Zn^{2+}-permeable GluR2-lacking α-amino-3-hydroxy-5-methyl-4-isoxazolepropionate (AMPA) receptors [8, 9]. Because intracellular (cytosolic) Zn^{2+} concentration (~ 100 pM) is much lower than Ca^{2+} concentration (~ 100 nM) [10, 11], Zn^{2+} toxicity is more critical for glutamate excitotoxicity than Ca^{2+} toxicity [12–15]. Even in cognitive activity via synaptic plasticity, excess influx of extracellular Zn^{2+} is more critical for cognitive decline than that of extracellular Ca^{2+} [16–18].

Alzheimer's disease (AD) is the most common cause of dementia and has a preclinical phase of 20–30 years before clinical onset [19, 20]. Amyloid β (Aβ) accumulation, the hallmark pathology of AD, is believed to play an upstream role in AD pathogenesis. Through mechanisms that are uncertain, Aβ oligomers can lead to cognitive decline in the pre-dementia stage of AD [21, 22]. The soluble forms of $A\beta_{1-42}$ are the most toxic species that can cause neuronal damage in the brains [23]. On the other hand, Zn^{2+} has been implicated in

✉ Atsushi Takeda
takedaa@u-shizuoka-ken.ac.jp

[1] Department of Neurophysiology, School of Pharmaceutical Sciences, University of Shizuoka, 52-1 Yada, Suruga-ku, Shizuoka 422-8526, Japan

[2] The Florey Institute of Neuroscience and Mental Health, The University of Melbourne, Parkville, VIC 3052, Australia

AD pathogenesis by inducing Aβ oligomerization [24, 25]. We have reported that $A\beta_{1–42}$ takes Zn^{2+} as a cargo into the dentate granule neurons in the normal brain and transiently affects memory acquisition via impairment of LTP induction in the normal brain [26, 27].

Our idea is that $A\beta_{1–42}$-induced increase in intracellular Zn^{2+} is neurotoxic; free Zn^{2+} is neurotoxic in dentate granule cells rather than $A\beta_{1–42}$ itself because intracellular and extracellular Zn^{2+} chelators rescue $A\beta_{1–42}$-induced memory deficit via attenuated LTP induction [26]. This means that memory does not form 1 h after learning; rats do not recognize a new object 1 h after learning familiarized objects. On the other hand, 3-day-maintained LTP underlies 3-day-old space recognition memory [28]. In the present study, we tested whether $A\beta_{1–42}$-induced increase in intracellular Zn^{2+} affects 3-day-old memory. The aim of the present study is to test whether $A\beta_{1–42}$-induced increase in intracellular Zn^{2+} causes not only anterograde amnesia [26, 27] but also retrograde amnesia and also whether $A\beta_{1–42}$-induced retrograde amnesia is rescued by controlling the increase in toxic Zn^{2+} released from $A\beta_{1–42}$ in dentate granule cells by Zn^{2+} chelators or metallothionein synthesis.

Materials and Methods

Animals and Chemicals

Male Wistar rats (15–20 weeks of age) were purchased from Japan SLC (Hamamatsu, Japan). Rats were housed under the standard laboratory conditions (23 ± 1 °C, 55 ± 5% humidity) and had access to tap water and food ad libitum. All the experiments were performed in accordance with the Guidelines for the Care and Use of Laboratory Animals of the University of Shizuoka that refer to the American Association for Laboratory Animals Science and the guidelines laid down by the NIH (NIH Guide for the Care and Use of Laboratory Animals) in the USA. The Ethics Committee for Experimental Animals in the University of Shizuoka has approved this work.

Synthetic human $A\beta_{1–42}$ and $A\beta_{1–40}$ were purchased from ChinaPeptides (Shanghai, China). ZnAF-2DA ($K_d = 2.7 \times 10^{-9}$ M for zinc), a membrane-permeable zinc indicator, was kindly supplied from Sekisui Medical Co., LTD (Hachimantai, Japan). ZnAF-2DA is taken up into the cells through the cell membrane and is hydrolyzed by esterase in the cytosol to yield ZnAF-2, which cannot permeate the cell membrane [29, 30]. Calcium Orange AM, a membrane-permeable calcium indicator, was purchased from Molecular Probes, Inc. (Eugene, OR). These fluorescence indicators were dissolved in dimethyl sulfoxide (DMSO) and then diluted to artificial cerebrospinal fluid (ACSF) containing 119 mM NaCl, 2.5 mM KCl, 1.3 mM $MgSO_4$, 1.0 mM NaH_2PO_4, 2.5 mM $CaCl_2$, 26.2 mM $NaHCO_3$, and 11 mM D-glucose (pH 7.3).

In Vivo Dentate Gyrus LTP in Freely Moving Rats

Male rats were anesthetized with chloral hydrate (400 mg/kg) and placed in a stereotaxic apparatus. A bipolar stimulating electrode and a monopolar recording electrode made of tungsten wire attached to an injection cannula (internal diameter, 0.15 mm; outer diameter, 0.35 mm) were positioned stereotaxically so as to selectively stimulate the perforant pathway while recording in the dentate gyrus. The electrode stimulating the perforant pathway was positioned 8.0 mm posterior to the bregma, 4.5 mm lateral, 3.0–3.5 mm inferior to the dura. A recording electrode was implanted ipsilaterally 4.0 mm posterior to the bregma, 2.5 mm lateral, and 3.0–3.5 mm inferior to the dura. Rats were allowed to recover for 1 week in individual home cages.

LTP experiments were performed in freely moving and unanesthetized rats. All the stimuli were biphasic square wave pulses (200 μs width) and their intensities were set at the current that evoked 40% of the maximum population spike (PS) amplitude. Test stimuli (0.05 Hz) were delivered at 20-s intervals to monitor PS amplitude. After stable baseline recording for at least 30 min, LTP was induced by delivery of high-frequency stimulation (HFS; 5 trains of 400 pulses at 400 Hz separated by 2 min). One hour-6 days later, PS amplitudes were measured for 10 min, averaged, and expressed as percentages of the mean PS amplitude measured during the 30-min baseline period prior to LTP induction, which was expressed as 100%. Judging from the PS amplitude, in the present study, it is estimated that LTP was induced at the medial perforant pathway-DGC synapses. When the medial perforant pathway is electrically stimulated, it produces a characteristic waveform of evoked field excitatory postsynaptic potential (fEPSP) superimposed by a PS [28].

Y-Maze Test

The maze apparatus was made of acrylic plates covered with a polypropylene sheet, with three arms placed symmetrically at a 120° angle from one another. The walls were 31 cm high, the arms 17 cm wide and 49 cm long. Removable walls that were made of acrylic plates decorated with a pattern of stripe or dot were inserted into an arm to make a novel space. Two objects (cups, 11 cm and 17 cm high) were used as cues to discriminate between the familiarized spaces and a novel space.

The recognition memory test was designed based on the evidence that rats tend to explore new environments. In the training trial (the first trial), one arm was removed from the maze apparatus and a rat was placed to the joint (triangle) area and allowed to explore two arms without removable wall for 5 min. The maze apparatus exploration was used as a context

habituation trial for the recognition memory task. One day later, the rat was placed in the join area of the maze in the same manner and allowed to explore the two arms in the second trial for 5 min. In the second trial, the identical object was placed closely to the back wall in the two arms. Two days later, agents in vehicle were bilaterally injected via injection cannulas (internal diameter, 0.15 mm; outer diameter, 0.35 mm) into the dentate gyrus at the rate of 0.25 μl/min for 8 min. One day later (3 days after the second trial), the test trial was performed for 3 min. One arm as a novel space was added to the maze apparatus and the rat was placed in the join area of the maze in the same manner and allowed to explore all of three arms. A removable wall was placed in one arm to make a new environment and a novel object was placed closely to the back wall in the arm. Other two arms were the same environment as the second trial. Behavior of rats was recorded with a video camera during the training and the test, and then two persons independently measured exploratory time in each arm and the averaged time was used. A recognition index calculated for each rat was expressed by the ratio $T_C/(T_A + T_B + T_C)$ [T_A and T_B = time spent to explore the familiarized arms; T_C = time spent to explore the novel arm]. We cleaned the maze arms and objects between trials with 70% ethanol solution.

In Vivo Imaging of Intracellular Zn^{2+} and Ca^{2+}

The rats were anesthetized with chloral hydrate (400 mg/kg) and individually placed in a stereotaxic apparatus. The skull was exposed, a burr hole was drilled, and injection cannulae (CXMI-6, EICOM Co.) were implanted into the dentate molecular layer of the right and left hippocampi. Thirty minutes after the surgical operation, agents in saline containing ZnAF-2DA (100 μM) were bilaterally injected via cannulae at the rate of 0.25 μl/min for 8 min. Five minutes after injection, the injection cannulas were slowly pulled out the brain in 3 min and the rats were decapitated. The brain was quickly removed and immersed in ice-cold choline-ACSF containing 124 mM choline chloride, 2.5 mM KCl, 2.5 mM $MgCl_2$, 1.25 mM NaH_2PO_4, 0.5 mM $CaCl_2$, 26 mM $NaHCO_3$, and 10 mM glucose (pH 7.3) to avoid neuronal excitation. Coronal brain slices (400 μm) were prepared using a vibratome ZERO-1 (Dosaka, Kyoto, Japan) in an ice-cold choline-ACSF. The brain slices were transferred to a chamber filled with ACSF, loaded for 30 min with 2 μM calcium orange AM in ACSF to identify the dentate gyrus, and washed out with ACSF for 10 min. The brain slices were transferred to a recording chamber filled with ACSF. The fluorescence of ZnAF-2 (laser, 488 nm; emission, 505–530 nm) and calcium orange (laser, 543 nm; emission, above 560 nm) was measured with a confocal laser-scanning microscopic system LSM 510 (Carl Zeiss), equipped with an inverted microscope (Axiovert 200 M, Carl Zeiss). Region of interest was set in the dentate granule cell layer of the dentate gyrus. All solutions used in the experiments were continuously bubbled with 95% O_2 and 5% CO_2.

To obtain the best fluorescence images and measure the difference in fluorescence intensity exactly, we first checked the relationship between the gain (fluorescence sensitivity) and fluorescence intensity and then carefully decided the best gain for measuring the exact changes in fluorescence intensity. This decision was separately performed in all experiments. We have confirmed that fluorescence intensity is not saturated in all of fluorescence images.

Data Analysis

Student's paired *t* test was used for comparison of the means of paired data. For multiple comparisons, differences between treatments were assessed by one-way ANOVA or two-way repeated measures ANOVA followed by post-hoc testing using the Tukey's test (the statistical software, GraphPad Prism 5). A value of $p < 0.05$ was considered significant. Data were expressed as means ± standard error. The results of statistical analysis are described in each figure legend.

Results

Exogenous Zn^{2+} Impairs Maintained LTP and Memory

Space memory is retained via maintaining LTP at the medial perforant pathway-dentate granule cell synapses and this retention requires intracellular Zn^{2+} signaling in dentate granule cells [28]. On the other hand, this retention is affected by intracellular Zn^{2+} dysregulation via extracellular Zn^{2+} influx [18]. On the other hand, it is estimated that Zn-Aβ_{1-42} oligomers formed in the extracellular compartment is rapidly taken up into dentate granule cells compared with extracellular Zn^{2+}, resulting in rapid production of toxic Zn^{2+} in dentate granule cells in vivo [27]. Thus, extracellular Zn-Aβ_{1-42} becomes more toxic in dentate granule cells than extracellular Zn^{2+} when the two are taken up into the cells. To verify this idea, toxic dose was compared between $ZnCl_2$ and Aβ. $ZnCl_2$ (50–250 μM, 2 μl) was locally injected into the dentate gyrus of freely moving rats 2 days after LTP induction. Six-day-maintained LTP was impaired by 250 μM Zn^{2+}, but not by 50 μM Zn^{2+} (Fig. 1a–c).

Memory retention was assessed by the Y maze test. If rats forget the two familiarized arms, the recognition index is approximately 33% in the test to explore the three arms equally. The control rats preferentially explored the novel arm unlike

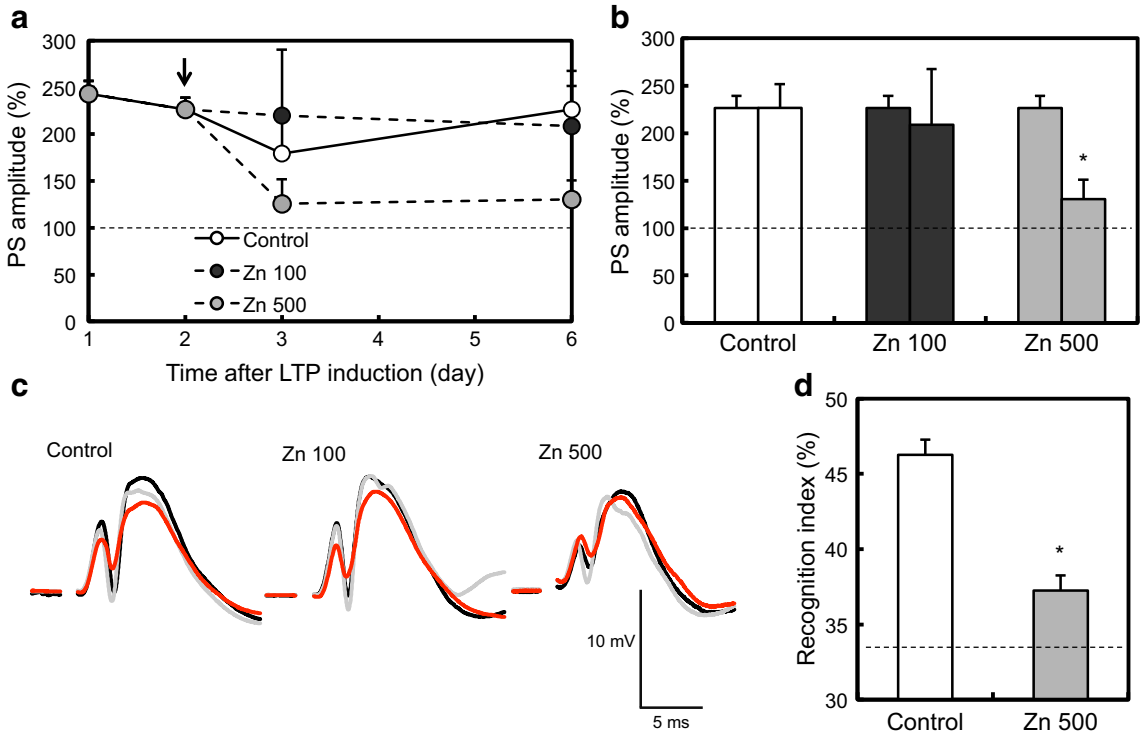

Fig. 1 Exogenous Zn^{2+} impairs maintained LTP and memory. **a** The PS amplitude was recorded 1 h, 1 day, 2 days, 3 days, and 6 days after LTP induction. Two days after LTP induction, vehicle (saline, control, $n = 6$), 100 pmol (50 μM $ZnCl_2$, $n = 4$), and 500 pmol $ZnCl_2$ (250 μM $ZnCl_2$, $n = 13$) in vehicle (2 μl) were injected via an injection cannula attached to a recording electrode into the dentate gyrus at the rate of 0.25 μl/min for 8 min as indicated by the arrow. **b** Each bar and line (the mean ± SEM) represent PS amplitude 2 d and 6 d after LTP induction. *$p < 0.05$ vs. control 6 days (Tukey's test). **c** Representative fEPSP recordings were shown (red, before LTP induction, gray; 2 days after LTP induction, black; 6 days after LTP induction). **d** A rat was placed in the joint (triangle) area of the Y-maze and allowed to explore two identical arms. One day later, the rat was placed in the same manner in the two arms with two identical objects. Two days later, vehicle ($n = 14$) and 500 pmol $ZnCl_2$ (250 μM $ZnCl_2$, $n = 15$) in vehicle (2 μl) were bilaterally injected into the dentate gyrus via injection cannulae in the same manner. One day later, the test was performed in the Y-maze with one novel arm in the presence of a novel object. *$p < 0.05$ vs. control (*t* test)

Zn^{2+}-injected rats because of recognizing the familiarized arms and showed a high recognition index in the test. Three-day-old space recognition memory was impaired by injection of Zn^{2+} (Fig. 1d).

$A\beta_{1–40}$ Impairs Maintained LTP via No Increase in Intracellular Zn^{2+}

$A\beta_{1–40}$ was locally injected into the dentate gyrus of freely moving rats 2 days after LTP induction in the same manner as the case of $ZnCl_2$. Interestingly, 2-day-maintained LTP was attenuated after only 25 μM $A\beta_{1–40}$ (2 μl) injection (Fig. 2a) and 6-day-maintained LTP was significantly impaired (Fig. 2b). $A\beta_{1–40}$-induced impairment of maintained LTP was rescued by co-injection of CaEDTA, an extracellular Zn^{2+} chelator, but not by co-injection of ZnAF-2DA, an intracellular Zn^{2+} chelator (Fig. 2).

To assess $A\beta_{1–40}$-mediated Zn^{2+} dynamics under the present experimental condition, $A\beta_{1–40}$ was co-injected with ZnAF-2DA into the dentate gyrus. $A\beta_{1–40}$ did not increase intracellular Zn^{2+} level in the dentate granule cell layer (Fig. 4a, c).

$A\beta_{1–42}$ Impairs Maintained LTP and Memory via Increase in Intracellular Zn^{2+}

$A\beta_{1–42}$ was also locally injected into the dentate gyrus of freely moving rats 2 days after LTP induction in the same manner as the case of $ZnCl_2$. Two-day-maintained LTP was also attenuated after only 25 μM $A\beta_{1–42}$ (2 μl) injection (Fig. 3a) and 6-day-maintained LTP was significantly impaired (Fig. 3b). $A\beta_{1–42}$-induced impairment of maintained LTP was rescued by either co-injection of CaEDTA or ZnAF-2DA (Fig. 3). When $A\beta_{1–42}$ was co-injected with ZnAF-2DA into the dentate gyrus, $A\beta_{1–42}$ increased intracellular Zn^{2+} level only in the dentate gyrus (Fig. 4b, d), but not in the hippocampal CA1 and CA3 (data not shown). Three-day-old memory was impaired by local injection of $A\beta_{1–42}$ into dentate gyrus, while rescued by co-injection of either CaEDTA or ZnAF-2DA (Fig. 4e).

Intraperitoneal (i.p.) injection of dexamethasone, a metallothionein (MT) inducer, increases MT-I mRNA in the brain, but not MT-III mRNA [31]. It is estimated that dexamethasone-induced MTs buffer increase in

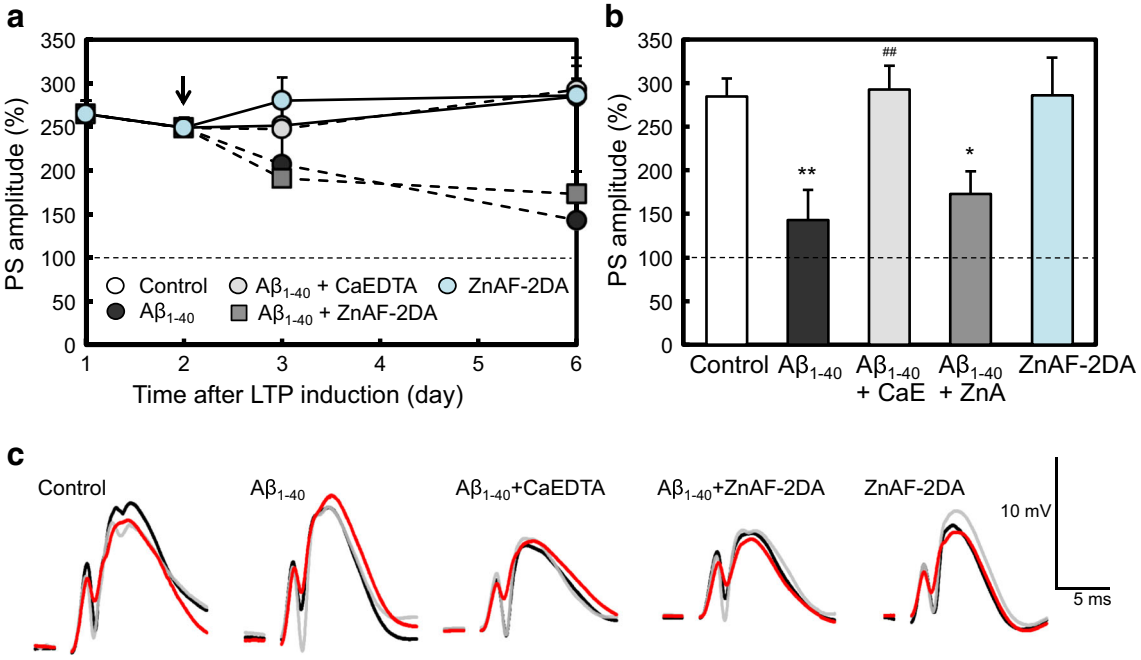

Fig. 2 $A\beta_{1–40}$-induced impairment of maintained LTP and its rescue by CaEDTA. **a** Two days after LTP induction, vehicle (saline, control, $n = 13$), $A\beta_{1–40}$ (25 μM, $n = 7$), $A\beta_{1–40}$ + CaEDTA (CaE, 10 mM, $n = 4$), $A\beta_{1–40}$ + ZnAF-2DA (ZnA, 100 μM, $n = 6$), and ZnAF-2DA ($n = 4$) in vehicle (2 μl) were injected via an injection cannula attached to a recording electrode into the dentate gyrus at the rate of 0.25 μl/min for 8 min as indicated by the arrow. **b** Each bar and line (the mean ± SEM) represent PS amplitude 6 days after LTP induction. $^{*}p < 0.05$, $^{**}p < 0.01$ vs. control; $^{\#\#}p < 0.01$ vs. $A\beta_{1–40}$ (Tukey's test). **c** Representative fEPSP recordings were shown (red, before LTP induction, gray; 2 days after LTP induction, black; 6 days after LTP induction)

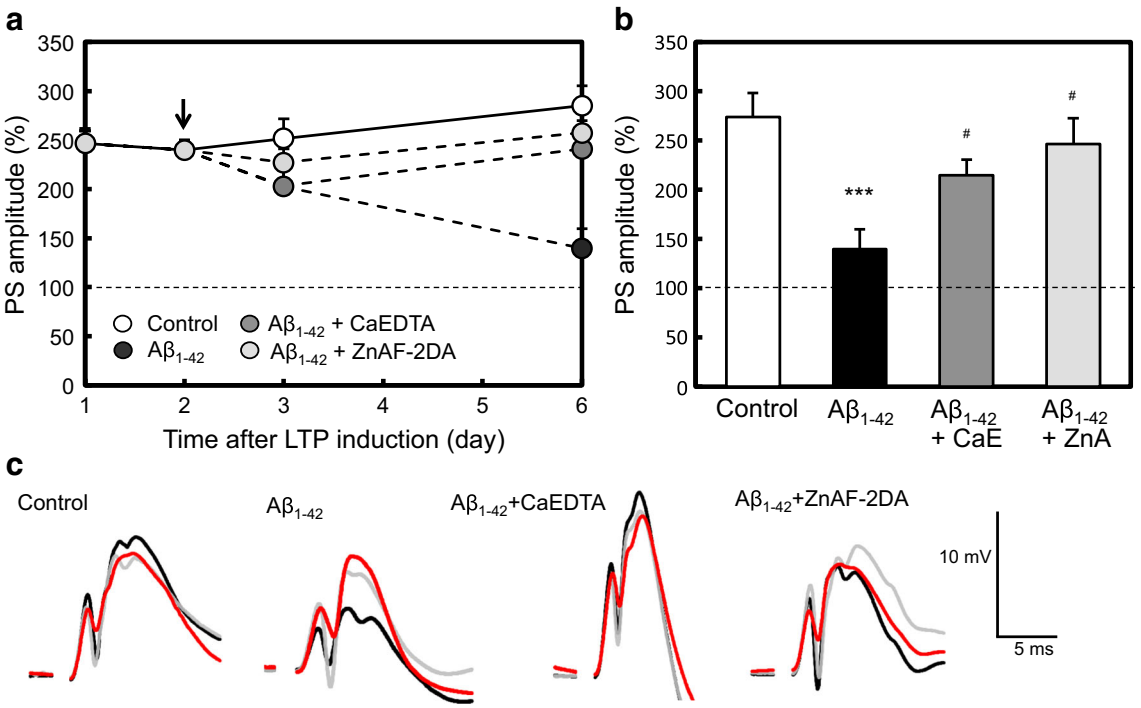

Fig. 3 $A\beta_{1–42}$-induced impairment of maintained LTP and its rescue by CaEDTA and ZnAF-2DA. **a** Two days after LTP induction, vehicle (saline, control, $n = 13$), $A\beta_{1–42}$ (25 μM, $n = 12$), $A\beta_{1–42}$ + CaEDTA (CaE, 10 mM, $n = 6$), and $A\beta_{1–42}$ + ZnAF-2DA (ZnA, 100 μM, $n = 5$) in vehicle (2 μl) were injected via an injection cannula attached to a recording electrode into the dentate gyrus at the rate of 0.25 μl/min for 8 min as indicated by the arrow. **b** Each bar and line (the mean ± SEM) represent PS amplitude 6 days after LTP induction. $^{***}p < 0.001$ vs. control; $^{\#}p < 0.05$ vs. $A\beta_{1–42}$ (Tukey's test). **c** Representative fEPSP recordings were shown (red, before LTP induction, gray; 2 days after LTP induction, black; 6 days after LTP induction)

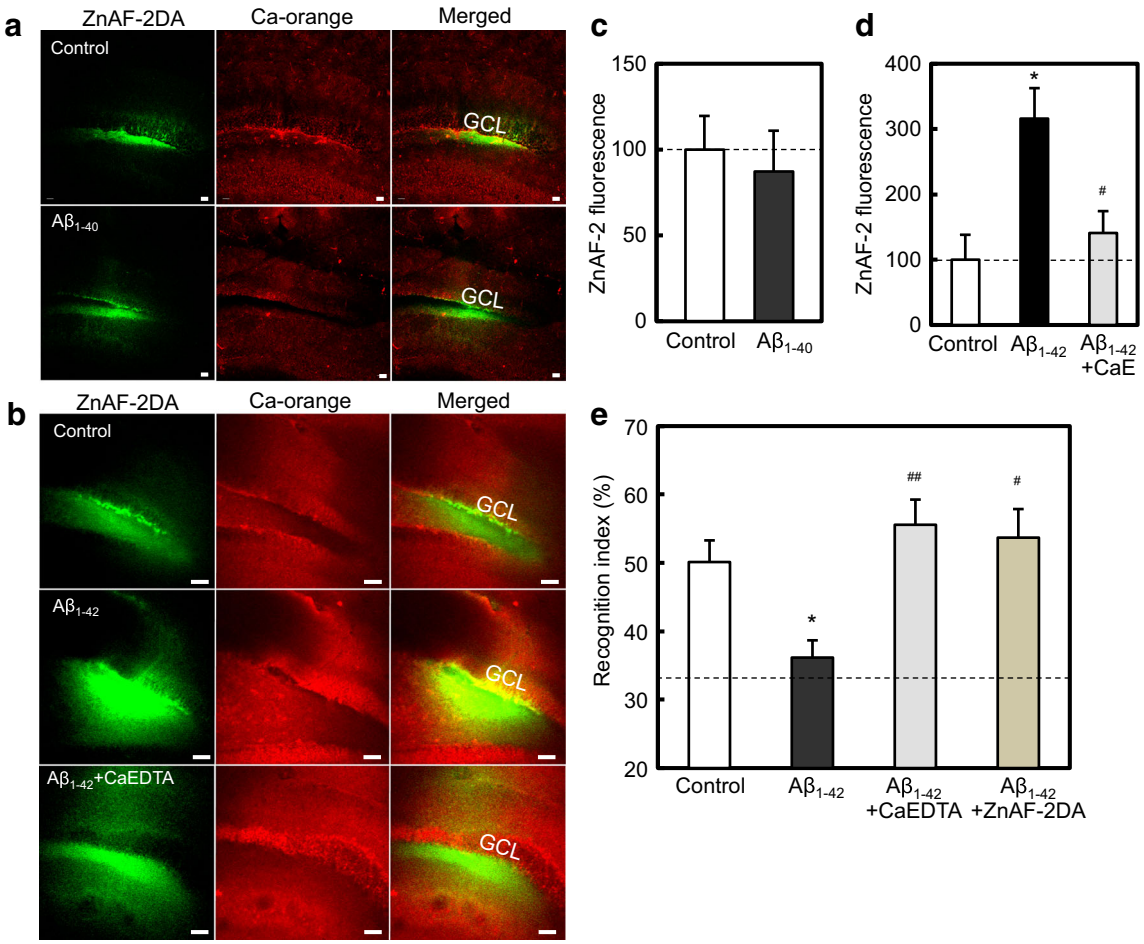

Fig. 4 In vivo Zn^{2+} uptake after injection of $A\beta_{1–40}$ and $A\beta_{1–42}$ into the dentate gyrus and rescue of $A\beta_{1–42}$-induced retrograde amnesia by Zn^{2+} chelators. **a** Intracellular Zn^{2+} images were determined in the dentate gyrus 5 min after bilateral injection of saline ($n = 7$) and 25 μM $A\beta_{1–40}$ in saline ($n = 7$) containing ZnAF-2DA (100 μM) via injection cannulae into the dentate gyrus at the rate of 0.25 μl/min for 8 min. **b** Intracellular Zn^{2+} images were also determined in the dentate gyrus 5 min after bilateral injection of saline ($n = 15$), 25 μM $A\beta_{1–42}$ in saline ($n = 8$), and 25 μM $A\beta_{1–42}$ + 10 mM CaEDTA (CaE) in saline ($n = 5$). **c**, **d** Quantitation of intracellular Zn^{2+} levels in the dentate granule cell layer (GCL) determined with intracellular ZnAF-2, which is represented by the ratio to the control ($n = 8$) without 25 μM Aβ in saline expressed as 100%. $^{*}p < 0.05$ vs. control, $^{\#}p < 0.05$ vs. $A\beta_{1–42}$. **e** A rat was placed in the joint (triangle) area of the Y-maze and allowed to explore two identical arms. One day later, the rat was placed in the same manner in the two arms with two identical objects. Two days later, vehicle ($n = 9$), $A\beta_{1–42}$ (25 μM, $n = 6$), $A\beta_{1–42}$ + CaEDTA (10 mM, $n = 7$), and $A\beta_{1–42}$ + ZnAF-2DA (100 μM, $n = 5$) in vehicle (2 μl) were bilaterally injected into the dentate gyrus via injection cannulae. One day later, the test was performed in the Y-maze with one novel arm in the presence of a novel object. $^{*}p < 0.05$ vs. control; $^{\#}p < 0.05$, $^{\#\#}p < 0.01$ vs. $A\beta_{1–42}$ (Tukey's test)

intracellular Zn^{2+} [32, 33] and capture Zn^{2+} released from $A\beta_{1–42}$ in dentate granule cells [34]. To assess the effect of MT induction under the present experimental condition, dexamethasone was i.p. injected once a day for 2 days and $A\beta_{1–42}$ was injected 24 h after dexamethasone injection. $A\beta_{1–42}$-induced impairment of maintained LTP was rescued by the preinjection of dexamethasone (Fig. 5), which blocked $A\beta_{1–42}$-induced increase in intracellular Zn^{2+} in the dentate granule cell layer (Fig. 6). The preinjection of dexamethasone had no effects on maintained LTP (Fig. 5) and intracellular Zn^{2+} level in the control dentate granule cell layer (Fig. 6).

Discussion

It has been reported that the formation of F-actin in dentate granule cells is essential for LTP maintenance via structural synapse enlargement [35, 36]. The increased amount of F-actin and its newly remodeled organization via calcium/calmodulin-dependent protein kinase II (CaMKII) provide new binding sites for many other postsynaptic proteins [37]. Newly synthesized LTP-related proteins can be captured at the new binding sites, sustaining the potentiated state for a long term. The location of CaMKII is crucial for its function [38, 39]. Kim et al. [40] report the importance of the interplay between the kinase and structural function of CaMKII in

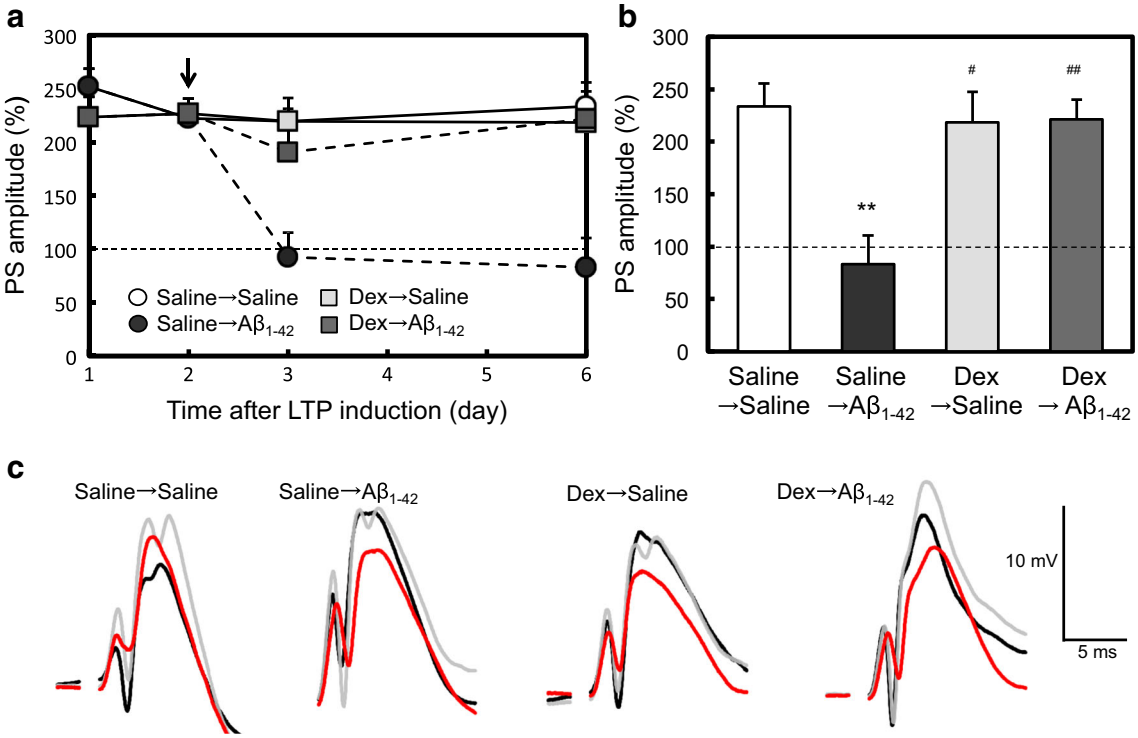

Fig. 5 $A\beta_{1–42}$-induced impairment of maintained LTP and its rescue by a MT inducer. **a** Two hours after LTP induction, vehicle and dexamethasone sodium phosphate (DEX, 10 mg/kg) in vehicle was i.p. injected into rats once a day for 2 days. Twenty-four hours later, vehicle (saline) and $A\beta_{1–42}$ (25 μM) in vehicle (2 μl) were injected via an injection cannula attached to a recording electrode into the dentate gyrus at the rate of 0.25 μl/min for 8 min as indicated by the arrow. **b** Each bar and line (the mean ± SEM) represent PS amplitude 6 d after LTP induction. $^{**}p < 0.01$ vs. control (saline/saline, $n = 5$); $^{\#}p < 0.05$, $^{\#\#}p < 0.01$ vs. $A\beta_{1–42}$ (saline/$A\beta_{1–42}$, $n = 5$); Dex/saline, $n = 4$; Dex/$A\beta_{1–42}$, $n = 5$; (Tukey's test). **c** Representative fEPSP recordings were shown (red, before LTP induction, gray; 2 days after LTP induction, black; 6 days after LTP induction)

defining a time window permissive for synaptic plasticity. Glucocorticoid-induced rapid increase in intracellular Zn^{2+} decreases phosphorylated CaMKII level, resulting in attenuating LTP induction [41]. Zn^{2+} concentrates in the postsynaptic density (PSD) and is able to influence the recruitment of ProSAP/Shank proteins to PSDs in a family member-specific manner during the course of synaptogenesis, synapse maturation, and structural plasticity [42]. MT-III is an actin-binding protein [43] and participates in actin polymerization in epidermal growth factor-treated astrocytes, which requires Zn^{2+} [44]. Therefore, synaptic Zn^{2+} homeostasis is critical for plastic changes in synaptic function and structure. It is possible that F-actin formation, which may be sensitive to intracellular Zn^{2+} dysregulation [28], is disturbed by increase in Zn^{2+} released from $A\beta_{1–42}$ in dentate granule cells, resulting in not only anterograde amnesia [26, 27] but also retrograde amnesia.

It is estimated that Zn-$A\beta_{1–42}$ oligomers formed in the extracellular compartment become more toxic in dentate granule cells than extracellular Zn^{2+} because Zn-$A\beta_{1–42}$ is more rapidly taken up into dentate granule cells than extracellular Zn^{2+} [27]. To assess the difference in synapse toxicity, $ZnCl_2$ and Aβ were locally injected into the dentate gyrus of freely moving rats. Space recognition memory via maintained LTP were impaired by local injection of 250 μM $ZnCl_2$ (2 μl), but not by local injection of 50 μM $ZnCl_2$ (2 μl). In contrast, maintained LTP was impaired by injection of either $A\beta_{1–40}$ or $A\beta_{1–42}$ (25 μM, 2 μl) into the dentate gyrus. The involvement of Zn^{2+} dynamics in Aβ-induced impairments of maintained LTP and memory was assessed using extracellular and intracellular Zn^{2+} chelators. $A\beta_{1–40}$-induced impairment of maintained LTP was rescued by co-injection of CaEDTA, but not by co-injection of ZnAF-2DA, suggesting that $A\beta_{1–40}$ impairs maintained LTP via no increase in intracellular Zn^{2+}, which was also confirmed by no increase in intracellular ZnAF-2 fluorescence. Although $A\beta_{1–40}$ has lower affinity for Zn^{2+} than $A\beta_{1–42}$ (K_d of $A\beta_{1–40}$ = 0.1–60 μM; K_d of $A\beta_{1–42}$ = ~ 3–30 nM) [27, 45], it is estimated that micromolar $A\beta_{1–40}$ captures Zn^{2+} in the extracellular compartment and impairs maintained LTP via the undefined action of extracellular Zn-$A\beta_{1–40}$. Huang et al. report that extracellular Zn^{2+} induces the reversible oligomerization of $A\beta_{1–40}$ via forming salt bridges between peptide subunits [46]. It is reported that the production ratio of $A\beta_{1–40}$ to $A\beta_{1–42}$ is a ratio of 10:1 [47]. Maintained LTP and memory retention might be impaired by $A\beta_{1–40}$ via a mechanism that involves extracellular Zn^{2+}.

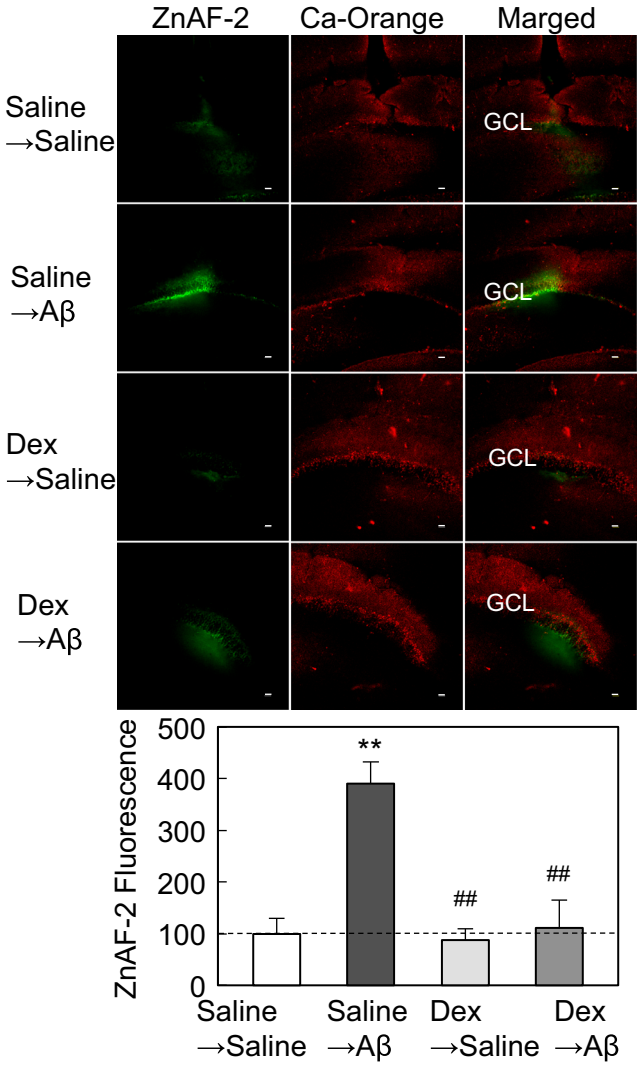

Fig. 6 Block of $A\beta_{1-42}$-induced increase in intracellular Zn^{2+} by a MT inducer. Saline and dexamethasone sodium phosphate (DEX, 10 mg/kg) in saline were i.p. injected into rats once a day for 2 days. Twenty-four hours later, saline and 25 μM $A\beta_{1-42}$ in saline containing 100 μM ZnAF-2DA (2 μl) were bilaterally injected into the dentate granule cell layer. Five minutes later, intracellular ZnAF-2 fluorescence were captured in the same manner as Fig. 4 (upper). Quantitation of intracellular Zn^{2+} levels in the dentate granule cell layer (GCL) determined with intracellular ZnAF-2, which is represented by the ratio to the control (saline/saline, $n = 5$) expressed as 100%. $^{**}p < 0.01$ vs. saline/saline, $^{\#\#}p < 0.01$ vs. saline/$A\beta_{1-42}$ ($n = 4$). DEX/saline, $n = 5$; Dex/Aβ, $n = 6$ (Tukey's test)

$A\beta_{1-42}$-induced impairment of memory retention via maintained LTP was rescued by co-injection of either CaEDTA or ZnAF-2DA, consistent with suppression of $A\beta_{1-42}$-induced increase in intracellular Zn^{2+} with CaEDTA. The present study indicates that maintained LTP and memory are impaired by $A\beta_{1-42}$-induced rapid Zn^{2+} influx into dentate granule cells. Aβ can bind up to 2.5 mol of Zn^{2+} in vitro [48]. When Zn^{2+} is ferried by $A\beta_{1-42}$ into dentate granule cells, the ferry transports Zn^{2+} at high speed (capacity) compared with free Zn^{2+} without the ferry. Taken together, the present data indicate that Zn-$A\beta_{1-42}$ is more rapidly taken up into dentate granule cells than free Zn^{2+} when extracellular Zn^{2+} is captured with $A\beta_{1-42}$. When $A\beta_{1-42}$ concentration reaches high picomolar (100~500 pM) in the extracellular compartment of the dentate gyrus, in vivo LTP induction is attenuated [27], suggesting that the interplay between high picomolar $A\beta_{1-42}$ and extracellular Zn^{2+} leads to rapid Zn-$A\beta_{1-42}$ uptake into dentate granule cells via an undefined mechanism.

Formation and propagation of misfolded aggregates of $A\beta_{1-42}$, rather than of $A\beta_{1-40}$, may contribute to AD pathogenesis, although structure of misfolded aggregates of $A\beta_{1-42}$ is not well understood [49]. C-Terminal carboxylate anion of $A\beta_{1-42}$ forms the C-terminal hydrophobic core, which accelerates neurotoxic oligomerization [50]. C-Terminal Ala42, which is absent in $A\beta_{1-40}$, forms a salt bridge with Lys28 to create a self-recognition molecular switch that is the $A\beta_{1-42}$-selective self-replicating amyloid-propagation machinery [51]. Extracellular Zn^{2+} rapidly enhances the aggregation property of $A\beta_{1-42}$. Characteristics of rapid Zn-$A\beta_{1-42}$ uptake into dentate granule cells might contribute to vulnerability of the dentate gyrus to aging and also AD [52, 53].

$A\beta_{1-42}$-induced impairment of maintained LTP was rescued by the preinjection of dexamethasone, which blocked $A\beta_{1-42}$-induced increase in intracellular Zn^{2+} in dentate granule cells. Intracellular Zn^{2+} dysregulation in dentate granule cells may impair hippocampus-dependent memory. The potential for metal chelation-based drug therapy using clioquinol, a copper/zinc ionophore and PBT2, a second-generation 8-hydroxyquinoline analog has been reported for AD [54, 55]. In contrast, MTs are non-toxic and functional as endogenous Zn^{2+} chelators, suggesting that MT induction may be an attractive strategy for defending $A\beta_{1-42}$-induced cognitive decline in the normal brain.

In conclusion, the present study indicates that $A\beta_{1-42}$-induced Zn^{2+} influx into dentate granule cells, which more readily occurs than free Zn^{2+}-induced Zn^{2+} influx, attenuates maintained LTP followed by retrograde amnesia. Furthermore, $A\beta_{1-42}$-induced retrograde amnesia was rescued by controlling the increase in toxic Zn^{2+} released from $A\beta_{1-42}$ in dentate granule cells by Zn^{2+} chelators or metallothionein synthesis. Therefore, controlling intracellular Zn^{2+} dysregulation may be a strategy for defending AD pathogenesis.

Compliance with Ethical Standards

Conflict of Interest The authors declare that they have no conflict of interest.

References

1. Bliss TV, Collingridge GL (1993) A synaptic model of memory: long-term potentiation in the hippocampus. Nature 361:31–39
2. Malenka RC, Nicoll RA (1999) Long-term potentiation-a decade of progress? Science 285:1870–1874

3. Nicoll RA, Malenka RC (1995) Contrasting properties of two forms of long-term potentiation in the hippocampus. Nature 377:115–118
4. Danbolt NC (2001) Glutamate uptake. Prog Neurobiol 65:1–105
5. Dong XX, Wang Y, Qin ZH (2009) Molecular mechanisms of excitotoxicity and their relevance to pathogenesis of neurodegenerative diseases. Acta Pharmacol Sin 30:379–387
6. Lai TW, Zhang S, Wang YT (2014) Excitotoxicity and stroke: identifying novel targets for neuroprotection. Prog Neurobiol 115:157–188
7. Lewerenz J, Maher P (2015) Chronic glutamate toxicity in neurodegenerative diseases-what is the evidence? Front Neurosci 9:469
8. Frederickson CJ, Koh JY, Bush AI (2005) The neurobiology of zinc in health and disease. Nat Rev Neurosci 6:449–462
9. Takeda A, Tamano H (2017) Impact of synaptic Zn^{2+} dynamics on cognition and its decline. Int J Mol Sci 18:2411
10. Sensi SL, Canzoniero LMT, Yu SP, Ying HS, Koh JY, Kerchner GA, Choi DW (1997) Measurement of intracellular free zinc in living cortical neurons: routes of entry. J Neurosci 15:9554–9564
11. Colvin RA, Bush AI, Volitakis I, Fontaine CP, Thomas D, Kikuchi K, Holmes WR (2008) Insights into Zn2+ homeostasis in neurons from experimental and modeling studies. Am J Physiol Cell Physiol 294:C726–C742
12. Colbourne F, Grooms SY, Zukin RS, Buchan AM, Bennett MV (2003) Hypothermia rescues hippocampal CA1 neurons and attenuates down-regulation of the AMPA receptor GluR2 subunit after forebrain ischemia. Proc Natl Acad Sci U S A 100:2906–2910
13. Liu S, Lau L, Wei J, Zhu D, Zou S, Sun HS, Fu Y, Liu F et al (2004) Expression of Ca(2+)-permeable AMPA receptor channels primes cell death in transient forebrain ischemia. Neuron 43:43–55
14. Weiss JH, Sensi SL (2000) Ca2+-Zn2+ permeable AMPA or kainate receptors: possible key factors in selective neurodegeneration. Trends Neurosci 365-71(2000):23
15. Weiss JH (2011) Ca permeable AMPA channels in diseases of the nervous system. Front Mol Neurosci 4:42
16. Suzuki M, Fujise Y, Tsuchiya Y, Tamano H, Takeda A (2015) Excess influx of Zn^{2+} into dentate granule cells affects object recognition memory via attenuated LTP. Neurochem Int 87:60–65
17. Takeda A, Koike Y, Osawa M, Tamano H (2018) Characteristic of extracellular Zn^{2+} influx in the middle-aged dentate gyrus and its involvement in attenuation of LTP. Mol Neurobiol 55:2185–2195
18. Takeda A, Tamano H, Hisatsune M, Murakami T, Nakada H, Fujii H (2018) Maintained LTP and memory are lost by Zn^{2+} influx into dentate granule cells, but not Ca^{2+} influx. Mol Neurobiol 1498-1508(2018):55
19. Nestor PJ, Scheltens P, Hodges JR (2004) Advances in the early detection of Alzheimer's disease. Nat Med10 Suppl 10:S34–S41
20. Querfurth HW, LaFerla FM (2010) Alzheimer's disease. N Engl J Med 362:329–344
21. Perrin RJ, Fagan AM, Holtzman DM (2009) Multimodal techniques for diagnosis and prognosis of Alzheimer's disease. Nature 461:916–922
22. Kepp KP (2016) Alzheimer's disease due to loss of function: a new synthesis of the available data. Prog Neurobiol 143:36–60
23. Iijima K, Liu HP, Chiang AS, Hearn SA, Konsolaki M, Zhong Y (2004) Dissecting the pathological effects of human Abeta40 and Abeta42 in Drosophila: a potential model for Alzheimer's disease. Proc Natl Acad Sci U S A 101:6623–6628
24. Bush AI, Pettingell WH, Multhaup G, d Paradis M, Vonsattel JP, Gusella JF, Beyreuther K, Masters CL et al (1994) Rapid induction of Alzheimer A beta amyloid formation by zinc. Science 265:1464–1467
25. Bush AI (2013) The metal theory of Alzheimer's disease. J Alzheimers Dis 33:S277–S281
26. Takeda A, Nakamura M, Fujii H, Uematsu C, Minamino T, Adlard PA, Bush AI, Tamano H (2014) Amyloid β-mediated Zn^{2+} influx into dentate granule cells transiently induces a short-term cognitive deficit. PLoS One 9:e115923
27. Takeda A, Tamano H, Tempaku M, Sasaki M, Uematsu C, Sato S, Kanazawa H, Datki ZL et al (2017) Extracellular Zn^{2+} is essential for amyloid $\beta_{1\text{-}42}$-induced cognitive decline in the normal brain and its rescu. J Neurosci 37:7253–7262
28. Tamano H, Minamino T, Fujii H, Takada S, Nakamura M, Ando M, Takeda A (2015) Blockade of intracellular Zn^{2+} signaling in the dentate gyrus erases recognition memory via impairment of maintained LTP. Hippocampus 25:952–962
29. Hirano T, Kikuchi K, Urano Y, Nagano T (2002) Improvement and biological applications of fluorescent probes for zinc, ZnAFs. J Am Chem Soc 124:6555–6562
30. Ueno S, Tsukamoto M, Hirano T, Kikuchi K, Yamada MK, Nishiyama N, Nagano T, Matsuki N et al (2002) Mossy fiber Zn^{2+} spillover modulates heterosynaptic *N*-methyl-*D*-aspartate receptor activity in hippocampal CA3 circuits. J Cell Biol 158:215–220
31. Palmiter RD, Findley SD, Whitmore TE, Durnam DM (1992) MT-III, a brain-specific member of the metallothionein gene family. Proc Natl Acad Sci U S A 89:6333–6337
32. Krężel A, Maret W (2006) Zinc buffering capacity of a eukaryotic cell at physiological pZn. J Biol Inorg Chem 11:1049–1062
33. Krężel A, Maret W (2017) The functions of metamorphic metallothioneins in zinc and copper metabolism. Int J Mol Sci 18. https://doi.org/10.3390/ijms18061237
34. Takeda A, Tamano H, Hashimoto W, Kobuchi S, Suzuki H, Murakami T, Tempaku M, Koike Y et al (2018) Novel defense by metallothionein induction against cognitive decline: from amyloid $\beta_{1\text{-}42}$-induced excess Zn^{2+} to functional Zn^{2+} deficiency. Mol Neurobiol 55:7775–7788. https://doi.org/10.1007/s12035-018-0948-5
35. Fukazawa Y, Saitoh Y, Ozawa F, Ohta Y, Mizuno K, Inokuchi K (2003) Hippocampal LTP is accompanied by enhanced F-actin content within the dendritic spine that is essential for late LTP maintenance in vivo. Neuron 38:447–460
36. Messaoudi E, Kanhema T, Soulé J, Tiron A, Dagyte G, da Silva B, Bramham CR (2007) Sustained Arc/Arg3.1 synthesis controls long-term potentiation consolidation through regulation of local actin polymerization in the dentate gyrus in vivo. J Neurosci 27:10445–10455
37. Okamoto K, Bosch M, Hayashi Y (2009) The roles of CaMKII and F-actin in the structural plasticity of dendritic spines: a potential molecular identity of a synaptic tag? Physiology (Bethesda) 24:357–366
38. Lee SJ, Escobedo-Lozoya Y, Szatmari EM, Yasuda R (2009) Activation of CaMKII in single dendritic spines during long-term potentiation. Nature 458:299–304
39. Halt AR, Dallapiazza RF, Zhou Y, Stein IS, Qian H, Juntti S, Wojcik S, Brose N et al (2012) CaMKII bind- ing to GluN2B is critical during memory consolidation. EMBO J 31:1203–1216
40. Kim K, Lakhanpal G, Lu HE, Khan M, Suzuki A, Hayashi MK, Narayanan R, Luyben TT et al (2015) A temporary gating of actin remodeling during synaptic plasticity consists of the interplay between the kinase and structural functions of CaMKII. Neuron 87:813–826
41. Suzuki M, Sato Y, Tamura K, Tamano H, Takeda A (2018) Rapid intracellular Zn^{2+} dysregulation via membrane corticosteroid receptor activation affects in vivo CA1 LTP. Mol Neurobiol. https://doi.org/10.1007/s12035-018-1159-9
42. Grabrucker AM, Knight MJ, Proepper C, Bockmann J, Joubert M, Rowan M, Nienhaus GU, Garner CC et al (2011) Concerted action of zinc and ProSAP/Shank in synaptogenesis and synapse maturation. EMBO J 30:569–581

43. El Ghazi I, Martin BL, Armitage IM (2006) Metallothionein-3 is a component of a multiprotein complex in the mouse brain. Exp Biol Med (Maywood) 231:1500–1506
44. Lee SJ, Cho KS, Kim HN, Kim HJ, Koh JY (2011) Role of zinc metallothionein-3 (ZnMt3) in epidermal growth factor (EGF)-induced c-Abl protein activation and actin polymerization in cultured astrocytes. J Biol Chem 286:40847–40856
45. Tõugu V, Karafin A, Palumaa P (2008) Binding of zinc(II) and copper(II) to the full-length Alzheimer's amyloid-beta peptide. J Neurochem 104:1249–1259
46. Huang X, Atwood CS, Moir RD, Hartshorn MA, Vonsattel JP, Tanzi RE, Bush AI (1997) Zinc-induced Alzheimer's Abeta1-40 aggregation is mediated by conformational factors. J Biol Chem 272:26464–26470
47. LaFerla FM, Green KN, Oddo S (2007) Intracellular amyloid-beta in Alzheimer's disease. Nat Rev Neurosci 8:499–509
48. Sensi SL, Paoletti P, Bush AI, Sekler I (2009) Zinc in the physiology and pathology of the CNS. Nat Rev Neurosci 10:780–791
49. Ahmed M, Davis J, Aucoin D, Sato T, Ahuja S, Aimoto S, Elliott JI, Van Nostrand WE et al (2010) Structural conversion of neurotoxic amyloid-beta(1-42) oligomers to fibrils. Nat Struct Mol Biol 17: 561–567
50. Masuda Y, Uemura S, Ohashi R, Nakanishi A, Takegoshi K, Shimizu T, Shirasawa T, Irie K (2009) Identification of physiological and toxic conformations in Abeta42 aggregates. Chembiochem 10:287–295
51. Xiao Y, Ma B, McElheny D, Parthasarathy S, Long F, Hoshi M, Nussinov R, Ishii Y (2015) Aβ(1-42) fibril structure illuminates self-recognition and replication of amyloid in Alzheimer's disease. Nat Struct Mol Biol 22:499–505
52. Small SA, Schobel SA, Buxton RB, Witter MP, Barnes CA (2011) A pathophysiological framework of hippocampal dysfunction in ageing and disease. Nat Rev Neurosci 12:585–601
53. Brickman AM, Khan UA, Provenzano FA, Yeung LK, Suzuki W, Schroeter H, Wall M, Sloan RP et al (2014) Enhancing dentate gyrus function with dietary flavanols improves cognition in older adults. Nat Neurosci 17:1798–1803
54. Lannfelt L, Blennow K, Zetterberg H, Batsman S, Ames D, Harrison J, Masters CL, Targum S et al (2008) Safety, efficacy, and biomarker findings of PBT2 in targeting Abeta as a modifying therapy for Alzheimer's disease: a phase IIa, double-blind, randomised, placebocontrolled trial. Lancet Neurol 7:779–786
55. Wang T, Wang CY, Shan ZY, Teng WP, Wang ZY (2012) Clioquinol reduces zinc accumulation in neuritic plaques and inhibits the amyloidogenic pathway in AβPP/PS1 transgenic mouse brain. J Alzheimers Dis 29:549–559